

RESEARCH

Open Access



High-frequency irreversible electroporation for cardiac ablation using an asymmetrical waveform

René van Es¹, Maurits K. Konings^{2*} , Bastiaan C. Du Pré¹, Kars Neven^{1,3,4}, Harry van Wessel⁶, Vincent J. H. M. van Driel⁵, Albert H. Westra², Pieter A. F. Doevendans^{1,7} and Fred H. M. Wittkamp¹

*Correspondence:
m.konings@umcutrecht.nl
² Dept. of Medical
Technology, University
Medical Center Utrecht,
Heidelberglaan 100, 3584
CX Utrecht, The Netherlands
Full list of author information
is available at the end of the
article

Abstract

Background: Irreversible electroporation (IRE) using direct current (DC) is an effective method for the ablation of cardiac tissue. A major drawback of the use of DC-IRE, however, are two problems: requirement of general anesthesia due to severe muscle contractions and the formation of bubbles containing gaseous products from electrolysis. The use of high-frequency alternating current (HF-IRE) is expected to solve both problems, because HF-IRE produces little to no muscle spasms and does not cause electrolysis.

Methods: In the present study, we introduce a novel asymmetric, high-frequency (aHF) waveform for HF-IRE and present the results of a first, small, animal study to test its efficacy.

Results: The data of the experiments suggest that the aHF waveform creates significantly deeper lesions than a symmetric HF waveform of the same energy and frequency ($p = 0.003$).

Conclusion: We therefore conclude that the use of the aHF enhances the feasibility of the HF-IRE method.

Background

Radiofrequency (RF) energy is the clinically used thermal modality to perform ablations for the treatment of cardiac arrhythmias. Thermal ablation, however, has many limitations and can lead to severe complications such as pulmonary vein stenosis, phrenic nerve palsy or in rare cases to paraesophageal fistula [1]. Besides possible complications, the long-term efficacy of RF ablation as a therapy for atrial fibrillation is only about 65%. Irreversible electroporation (IRE) may be a safer and more effective method for cardiac ablation [2]. Over the past decade, preclinical studies have shown that IRE is a safe and valuable method for cardiac ablation therapy [3–11]. With IRE, a direct current (DC) is applied between a skin patch and a multipolar circular catheter. The high-intensity electric field near the catheter electrodes produces pores in the phospholipid membranes of the cells, leading to an irreversible breakdown of membrane structure and function and finally to cell death [12].



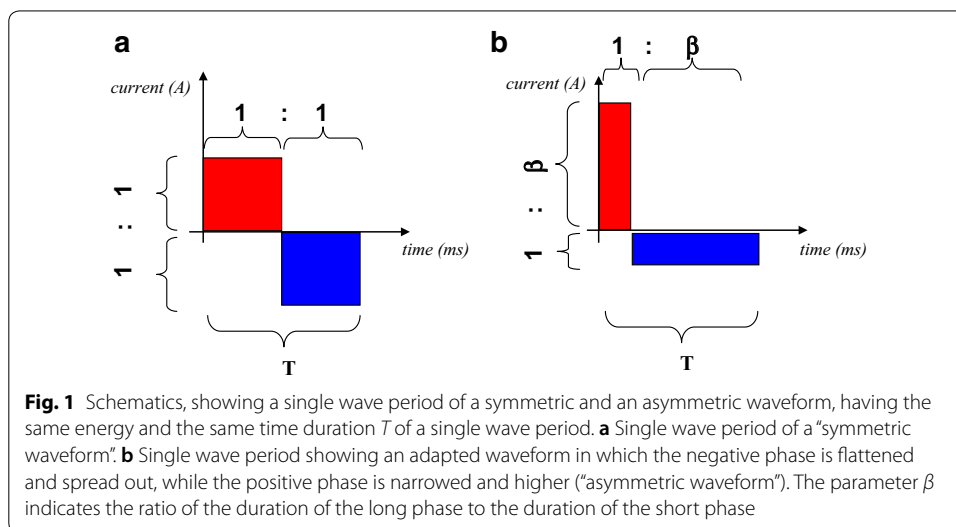
The direct current (DC), as used with IRE, leads to (skeletal) muscle contractions. When applying IRE in patients, the DC character of the applied current necessitates the use of general anesthesia. In addition, the DC current causes electrolysis on the electrode surfaces, thus producing bubbles containing the gaseous products from the electrolysis.

To prevent muscle stimulation, Arena et al. [13] studied the use of high-frequency (HF) alternating current for IRE and demonstrated the feasibility of HF-IRE for non-thermal ablation of brain tissue in rats without muscle contractions.

We have developed an *asymmetric* HF (aHF) waveform for IRE that is theoretically more effective than the (normal) symmetrical HF [14]. In this paper, our theoretical reasoning behind this asymmetrical waveform is explained, and *in vivo* experiments are presented that put this aHF waveform to the test. For clarity, throughout the paper, we will use the phrases “single wave period” and “wave train”, in which “single wave period” refers to a single short elementary wave period (having a duration of a few microseconds), whereas “wave train” refers to a series of many repeated contiguous single wave periods. These wave trains may themselves be repeated, so that the total treatment of a single patch of tissue may consist of a number of “wave trains”. The actual “asymmetry” of the aHF mentioned above takes place *within* each individual single wave period, as will be explained below using Fig. 1b.

The starting point for introducing our asymmetric waveform are remarks by, e.g., Son et al. indicating that electroporation is characterized by electrical creation of aqueous pores in cell membranes, in which the rate of the formation of these pores is strongly, and non-linearly, dependent on the transmembrane voltage [12, 15].

In our new method, we aim at exploiting this strongly non-linear, exponential, dependency on the transmembrane voltage, by applying an HF current pattern, in which, within each single wave period, one phase (e.g., the positive phase) has a much higher amplitude than the opposite phase. When compared to symmetrical HF, the high amplitude phase will then cause much more electroporation than the combined effect of both phases of symmetrical HF current, as explained below.



According to Krassowska et al. [12], the creation of electroporation pores in a membrane is proportional to $e^{(\Phi_m)^2}$, in which Φ_m is the transmembrane voltage. We hypothesize that it is favorable for pore formation to have the highest phases of the applied electric field “work in the same direction”, as with a DC pulse, instead of having equal values in alternating directions as is the case with the symmetrical waveform (see Fig. 1a). The underlying fundamental reason for our hypothesis is the non-linear nature of pore formation, i.e., the fact that pore formation is proportional to $e^{(\Phi_m)^2}$, which implies that, if the applied Φ_m would be increased with a factor 2, then the pore formation (and, consequently, cell death) would increase by a factor much larger than 2. Therefore, for enhancing the formation of electroporation pores, it is more effective to have a *higher* value of Φ_m during a *shorter* period of time, than a *lower* value of Φ_m that is spread out over a *longer* period of time.

Since the total charge released from the electrode during one single wave period (consisting of one positive and one negative phase) must always be exactly equal to zero (to avoid unwanted DC current), we introduce an asymmetric waveform (see Fig. 1b) in which, for each single wave period, the surface area of the positive phase is equal to the surface area of the negative phase. Given the above-mentioned fact that the creation of new electroporation pores in a membrane is proportional to $e^{(\Phi_m)^2}$, the positive phases of the asymmetrical wave, shown in Fig. 1b, are much more effective in pore creation compared to those of the symmetrical wave, shown in Fig. 1a, and hence the total net effect of the entire asymmetric wave is expected to work in one single direction (i.e., the direction of the positive phase), not unlike a DC pulse in that direction.

Therefore, *our first hypothesis* reads that the asymmetrical waveform (Fig. 1b) is more effective for IRE than the symmetrical waveform (Fig. 1a) of the *same energy and frequency*.

To set up a meaningful comparison of both waveforms, it is obvious to demand that the asymmetric and symmetric waveforms have the same energy within a single period of the wave. However, another obvious choice is to demand that, for both waveforms, each single (positive or negative) phase represents the same amount of charge (positive or negative) released from the electrodes, because, for frequencies well above 10 kHz, this amount of charge determines whether unwanted muscle spasms are evoked [13].

Therefore, *our second hypothesis* reads that the asymmetrical waveform (Fig. 1b) is more effective for irreversible electroporation than a symmetrical waveform of the same frequency if the positive (or negative) phase of the asymmetric waveform *has the same charge* as the positive (or negative) phase of the symmetric waveform. The charge of a positive phase of a waveform is represented by the area under the curve during that positive phase.

Furthermore, there are at least two boundary conditions that need to be met when designing an asymmetric waveform:

The *first boundary condition* is that the duration of one single period must be much shorter than 100 μ s (the chronaxie time of fast neurons [16]), to be able to avoid muscle spasms using the reasoning presented above.

The second boundary condition relates to the mechanism of building transmembrane voltages:

As explained by, e.g., Golberg et al. [17], the currently accepted theory is that, at the very beginning of each new (positive or negative) phase of a waveform representing the current injected from the electrode, a process starts that consists of at least two consecutive phases: (i) a brief initial phase during which the applied current causes the accumulation of charge (and hence the buildup of the transmembrane voltage Φ_m) on the membranes of cells, and (ii) the actual formation of pores in the membranes. Son et al. [18] present a simulation using an applied field strength of 1.5 kV/cm near the membrane, in which the first phase (i) has a duration of 0.7 μ s, after which a transmembrane voltage of 1.2 V is reached and a burst of pore formation ensues.

Therefore, the *second boundary condition* reads that duration of the shortest phase in the asymmetric wave must be much larger than the time needed to build up the transmembrane voltage of 1.2 V, in which the numbers used in the study by Son et al. serve as a guideline.

On the basis of mathematical analysis alone, it can be shown that if the symmetrical and the asymmetrical wave contain equal energy, then the *symmetrical wave has more charge* than the asymmetrical wave during a *single phase of one single period* of the wave. See [Appendix](#) for the mathematical derivation.

We therefore conclude that if *our first hypothesis* is confirmed by experiment, then *our second hypothesis* is confirmed automatically as well.

In the present study, the efficacy of both waveforms is analyzed on the basis of the size of the lesions that they produce.

Methods

High-frequency waveforms

The symmetric and asymmetric waveforms have been designed to comply with the two boundary conditions mentioned in the introduction, by choosing a frequency of 167 kHz.

The waveforms were generated using an HF pulse generator (HF-Puls 4, GBS Elektronik, Großerkmannsdorf, Germany). The generator was altered to enable the generation of asymmetrical pulses. The fact that we used an existing HF pulse generator as a starting point for our alterations, however, posed a limitation to the degree of asymmetry that could be achieved: the ratio of the duration of the long phase to the duration of the short phase, within a single wave period, could not exceed 2.6:1.

The asymmetric waveforms were composed in such a way that the asymmetric and symmetric waveforms have the same energy within a single period of the wave. In this way, the experiments are designed to test for the *first hypothesis* mentioned in "[Background](#)".

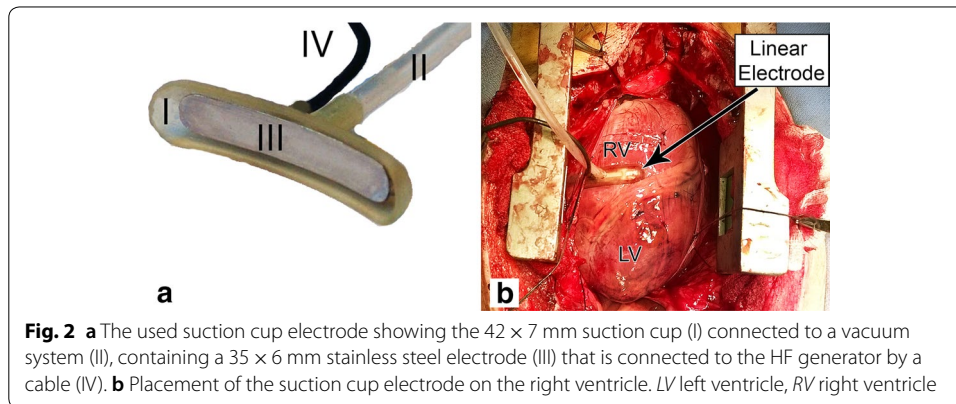
Two different types of experiments have been performed: (i) the main group of experiments, using ten consecutive wave trains (performed on animal groups M1 and M2, see [Table 1](#)), and an additional experiment (ii) using only one single wave train of high energy (performed on animal group E).

Animals

All animal experiments were performed with prior approval from the Animal Experimental Ethical Committee of the University Medical Center Utrecht (protocol number AVD115002015206).

Table 1 HF pulse protocol

	5 animals (model M)	
	Symmetrical	Asymmetrical ($\beta = 2.31$)
Positive voltage peak (V)	600	544
Negative voltage peak (V)	-600	-221
Frequency (kHz)	167	167
Number of wave trains	10	10
Interval (ms) between wave trains	400	400
Duration (ms) of single wave train	2	2
Delivered energy	10 × 20 J	10 × 20 J
Energy during one single wave period T	100%	100%
Charge during one single wave period T	100%	92%



In all models, 60–75 kg Dalling landrace pigs were premedicated with 10 mg/kg ketamine, 0.4 mg/kg midazolam and 0.5 mg atropine. Anesthesia was induced with 4 mg/kg thiopental sodium. During the rest of the procedure, 0.5 mg/kg/h midazolam, 2.5 mg/kg/h sufentanil and pancuronium bromide 0.1 mg/kg/h were administered. A midline sternotomy was performed and the pericardial sac was opened. Subsequently, the suction cup electrode (Fig. 2) was positioned on the right ventricle (RV) perpendicular to the left anterior descending coronary artery because of the visibility and ease of access. Then either one of the HF-IRE waveforms was applied (Table 1), and sutures were placed on both ends of the electrode. Successively, the suction cup electrode was repositioned 1 cm toward the apex and the other HF-IRE waveform was applied, and again sutures were placed.

Five animals for the main experiment (M)

Animal model M1

In two animals, 8 h after HF-IRE energy application, the animals were exsanguinated and the heart was removed for histological analysis.

Animal model M2

Three animals were pretreated with amiodarone, 800 mg/day, for 7 days before the procedure. After the administration of the HF-IRE, the pericardium and thorax were closed. Three weeks later the animals were exsanguinated and the heart was removed for histological analysis.

Additional animals for high-energy experiment (E)

In two additional animals, we repeated the experiments described above (experiment M), but all currents in the experiment (E) were two times stronger than the corresponding currents in the experiment (M), and, furthermore, the number of wave trains (10 wave trains in experiment (M), see Table 1), was reduced to just one single wave train. Besides these two changes in HF application, the experimental setup and follow-up time were the same as in model M2.

Histological analysis

In both groups, RV tissue containing the ablated area was isolated from the rest of the heart and fixated in a 4% formaldehyde solution for at least 3 days. From each lesion, two histological samples were taken at 1/3 and 2/3 along the length of the ablation site. Histological sections were prepared and stained with both hematoxylin and eosin (HE) and Elastic van Gieson (EvG). Lesion depth and RV wall thickness were scored by a blinded observer as described previously [8].

Statistical analysis

The impedance was calculated as the set peak-to-peak voltage divided by the measured peak-to-peak current. For the histology, the mean of the four measurements per animal per lesion was used for further analysis. A paired two tailed *t* test was used to compare lesion depth for both methods. A *p* value < 0.05 was considered to be statistically significant.

Results

The HF-IRE applications were successfully delivered in all experiments without medical complications. Minor skeletal muscle contractions were observed with all HF-IRE applications. Visual inspection of the ablation sites directly after IRE application always showed a hyperemic mark left by the suction cup. There were no signs of tissue heating (e.g., tissue whitening).

In Fig. 3, the current delivered via the electrodes during the experiments is rendered as a function of time, for the symmetric wave (left) and the asymmetric wave (right). The calculated impedance was not significantly different at $107 \pm 18 \Omega$ and $97 \pm 20 \Omega$ ($p = 0.137$) for the symmetric HF (sHF) and asymmetric HF (aHF) waveforms, respectively.

Histological analysis

In one animal of model E, due to adhesions, the epicardium was damaged during excision of the heart. This animal was excluded from further histological analysis. A total

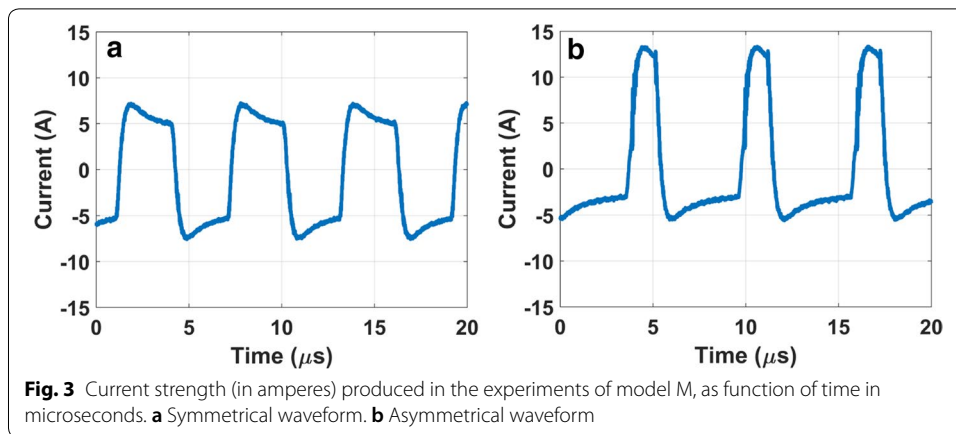


Table 2 Results

	Lesion depth (mm)		p-value
	Asymmetrical HF	Symmetrical HF	
Model M1 (n=2)	1.8 ± 0.4	1.2 ± 0.5	0.068
Model M2 (n=3)	2.7 ± 1.2	2.0 ± 0.9	0.065
Overall M (n=5)	2.3 ± 1.0	1.7 ± 0.8	0.003

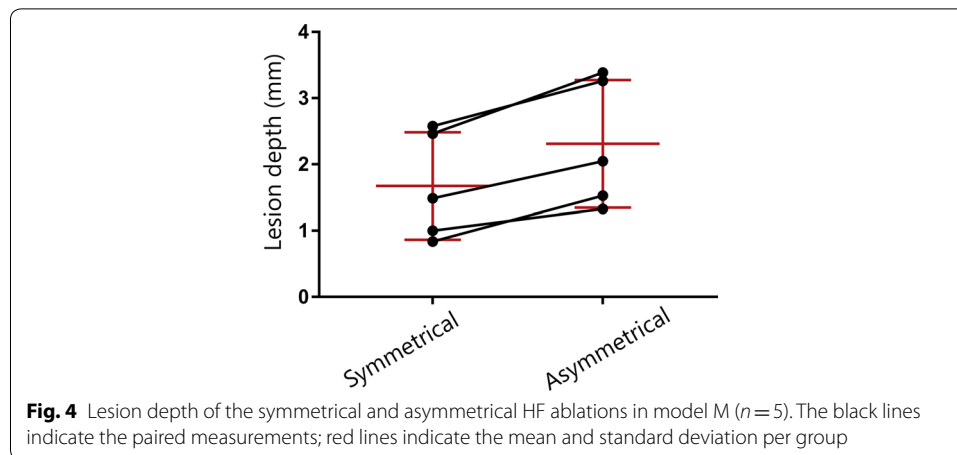
of 28 histological slides from seven animals were analyzed. There was no significant difference in the thickness of the RV myocardium at the lesion sites, 7.7 ± 2.2 mm and 5.9 ± 1.5 mm ($p = 0.15$) for the sHF and aHF sites, respectively.

Model M

In model M1, 8 h after HF-IRE, the sHF and aHF waveforms showed a lesion depth of 1.2 ± 0.3 mm and 1.8 ± 0.3 mm ($p = 0.068$), respectively. In model M2, 3 weeks after HF-IRE, the sHF and aHF showed a lesion depth of 2.0 ± 0.9 mm and 2.7 ± 1.2 mm ($p = 0.065$), respectively. See also Table 2. Overall, for all five animals of Model M, the asymmetrical waveform shows a significantly deeper average lesion depth of 2.3 ± 0.9 mm compared to the symmetrical waveform 1.7 ± 0.7 mm ($p = 0.003$), Fig. 4. The overall average relative lesion depth was significantly deeper for the asymmetrical waveform aHF lesions ($43.1 \pm 19.4\%$) than for the symmetrical waveform sHF lesions ($21.4 \pm 7.2\%$) ($p < 0.05$). With the sHF waveform, there were no transmural lesions (range: 11.6–31.6%). With the aHF waveform, there was one transmural lesion (range: 13.2–100%).

Model E

The average RV myocardial thickness was 10.0 ± 1.1 mm and 8.4 ± 4.6 mm ($p = 0.634$) in the sHF and aHF groups, respectively. In model E, 3 weeks after HF-IRE, the sHF and aHF showed a lesion depth 3.9 ± 0.4 mm and of 3.8 ± 1.5 mm ($p = 0.911$), respectively. The average relative lesion depths were $38.1 \pm 2.0\%$ and $55.0 \pm 9.3\%$ ($p = 0.281$) for the sHF and aHF lesions, respectively.



Discussion

In the present porcine study, we demonstrated the feasibility of a novel asymmetrical aHF waveform for IRE, and compared it directly to a conventional, symmetrical sHF waveform. This is the first time that an asymmetrical wave has been utilized for IRE ablation and has shown to be usable for non-thermal ablation of cardiac tissue. In the animals that received multiple low-energy HF-IRE application, the aHF waveform led to significantly deeper lesions than the sHF waveform. As a result, we conclude that the *first hypothesis* from “Background” has been confirmed, i.e., an asymmetrical high-frequency waveform creates deeper lesions than a symmetrical waveform of the same energy. In [Appendix](#), we show that if the *first hypothesis* is confirmed, then the *second hypothesis* (i.e., an asymmetric high-frequency waveform creates deeper lesions than a symmetric waveform having the same charge per phase) is confirmed automatically as well.

Our findings are in accordance with the strength–duration relation for the irreversible lesion of cardiomyocytes by high-intensity electric fields as presented by Prado et al. [15], in which the strength of the electric field necessary to kill 50% of the cells, E_{50} , was fitted to their measured data using $E_{50} = Kd^A + B$, in which d is the duration of the applied field, and $A = -0.54$, thus indicating a strongly non-linear relation between E_{50} and d .

In the two animals that received one single high-energy HF application, there was no significant difference between aHF and conventional HF, but both methods showed lesions of more than 4 mm deep. With all HF-IRE applications, we observed minor skeletal muscle contractions; these were however considerably less forceful than those observed with DC-IRE applications. A bench test of the HF generator revealed a small unintended low-frequency component (<500 Hz) in the waveform. This low-frequency wave is assumed to be responsible for the observed minor muscle contractions in the present in vivo experiments.

For the purpose of pulmonary vein isolation, lesions of a few millimeters deep are required to ensure a transmural ablation of the usually thin myocardial sleeves. The use of a single high-energy aHF-IRE application [high-energy experiment (E)] has been shown to be capable of producing lesions that are deep enough for pulmonary vein isolation. However, these lesions were created by applying the HF current between a skin

patch and an electrode in a suction cup. When applying this HF current between the skin patch and a circular multi-electrode catheter, due to the low resistance of blood, about 2/3 of the energy dissipates into the blood pool instead of the tissue. Therefore, when using a circular multi-electrode catheter instead of a suction cup, considerably higher currents will be required.

In this study, the aHF and sHF applications provoked extremely minor skeletal muscle contractions, especially compared to DC-IRE applications observed in previous studies [1–6]. For high frequencies, i.e., frequencies that are well above $1/T_{\text{chron}}$, in which T_{chron} is the chronaxie time, the neurostimulation threshold is essentially proportional to the frequency. Therefore, high frequencies, as used in the present study, are less likely to stimulate skeletal muscles.

To investigate whether or not bubble formation (due to electrolysis) takes place using our symmetric or asymmetric high-frequency protocols, we performed extensive testing in a saline bath and studied the surfaces of the electrodes during the pulses. No visible bubble formation on or near the electrode surfaces was found.

Limitations

The number of animals used for this pilot study was small; however, significant differences between the two study groups were obtained. We did not quantitatively assess skeletal muscle contraction, instead assessment was performed visually. Future studies on HF-IRE should incorporate measurements of peak acceleration to quantitatively assess skeletal muscle contractions.

Higher energies are required when using this HF technology for clinical ablation procedures. In the present study, we were unable to test higher energy settings due to limitation of the experimental generator.

Clinical perspective

The depth of the lesions created with the asymmetric HF waveform in these pilot experiments may not yet be sufficient for the creation of transmural scars in the ostia of the pulmonary veins. We expect that using a higher power and a higher value for β in the asymmetric pulse will create lesions suitable for pulmonary vein isolation. Besides the application of aHF-IRE for pulmonary vein isolation, other applications in the field of cardiac electrophysiology are possible, for example with epicardial approaches [7].

We expect that a substantially higher value for β in the asymmetric pulse will boost the efficacy of the aHF-IRE even further, thus making it a suitable alternative for DC-IRE, because aHF-IRE will avoid skeletal muscle contractions and gas bubble formation due to electrolysis; further studies are however required to prove this.

Irreversible electroporation using various waveforms is increasingly being investigated for the purpose of cardiac ablation. The first clinical trials have been performed using (pulsed) high-voltage waveform that used general anesthesia to avoid skeletal muscle stimulation [19]. Besides the present study, other research into symmetrical biphasic waveforms is being conducted [20]. In contrast to the present study, both approaches apply the pulses between multiple catheter electrodes, obviating the need for a skin patch. While the

approach could lead to less skeletal muscle stimulation, it may have ramifications for the size of the created lesions considering the resulting shape of the electric field.

Conclusion

The present study demonstrates that the novel asymmetric high-frequency waveform can create lesions in cardiac tissue. The data of the experiments also suggest that an asymmetric high-frequency waveform creates deeper lesions than a symmetric waveform of the same energy, or a symmetric waveform of the same charge.

Acknowledgements

We gratefully acknowledge Evelyn Velema, Marlijn Jansen, Grace Croft, Martijn van Nieuwburg and Joyce Visser for their help with the animal experiments.

Authors' contributions

RvE designed, planned, and executed the experiments, wrote "Methods" and "Results" sections, and co-edited the entire manuscript. MKK invented the asymmetric waveform method, defined its mathematical and physical foundations, wrote "Background" and "Discussion" sections as well as Appendix, and co-edited the entire manuscript. BDP, KN, HvW, and VvD all contributed to the setup and execution of the experiments and co-edited the manuscript. AHW made essential contributions to the design and prototyping of the new electronic equipment needed for the production of high-voltage asymmetric HF waves. PAD and FHW supervised and co-designed the experiments, and co-edited the manuscript. All authors read and approved the final manuscript.

Funding

Part of this research has been funded by Abbott Laboratories, Abbott Park, Illinois, USA.

Availability of data and materials

Not applicable.

Ethics approval and consent to participate

All animal experiments were performed with prior approval from the Animal Experimental Ethical Committee of the University Medical Center Utrecht. No patients or human volunteers have been involved in this study.

Consent for publication

Not applicable.

Competing interests

The authors declare that they have no competing interests. Part of this research has been funded by Abbott Laboratories, Abbott Park, Illinois, USA. A patent concerning the asymmetric waveform has been filed (ownership: Abbott, Illinois, USA. Inventor: Maurits K Konings).

Author details

¹ Div. Heart and Lungs, Dept. of Cardiology, University Medical Center Utrecht, Utrecht, The Netherlands. ² Dept. of Medical Technology, University Medical Center Utrecht, Heidelberglaan 100, 3584 CX Utrecht, The Netherlands. ³ Witten/Herdecke University, Witten, Germany. ⁴ Dept. of Electrophysiology, Alfried Krupp Krankenhaus, Essen, Germany. ⁵ Dept. of Cardiology, Haga Teaching Hospital, The Hague, The Netherlands. ⁶ Abbott, Veenendaal, The Netherlands. ⁷ Holland Heart House, Utrecht, The Netherlands.

Appendix

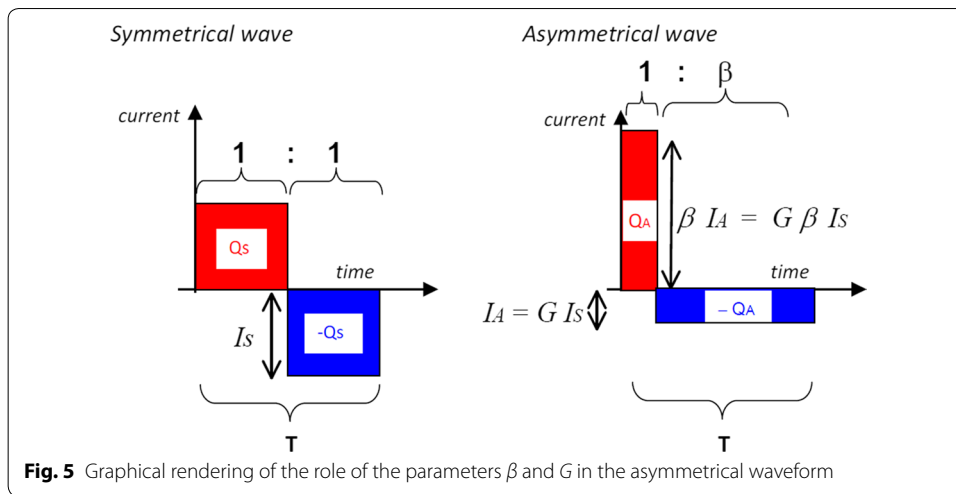
In this appendix, we show that, for all values of $\beta > 1$, the following statement is true: if the symmetrical and the asymmetrical wave contain equal energy, then the *symmetrical wave has more charge* than the asymmetrical wave during a *single phase of one single period* of the wave.

To prove the validity of this statement, we first calculate the amplitudes needed for the asymmetrical wave to let its energy be equal to the energy of the symmetrical wave.

Equal energy

Let I_S denote the amplitude of the symmetrical wave. The energy E_S that is released during a single period of the symmetrical wave then reads:

$$E_S = (I_S)^2 RT, \quad (1)$$



in which R is the resistance between the electrodes and T is the duration of a single period of the wave.

Let I_A denote the amplitude of the longest period of the asymmetrical wave (see Fig. 5), which can be tuned using a controllable gain factor G :

$$I_A = GI_S. \tag{2}$$

The longest phase of a single period of the asymmetrical wave has amplitude I_A and duration $T\beta/(1+\beta)$, and hence releases a charge equal to $I_A(T\beta)/(1+\beta)$ and an energy equal to

$$(I_A)^2 RT \beta / (1 + \beta). \tag{3}$$

However, the shortest phase of a single period of the asymmetrical wave has amplitude βI_A and duration $T/(1+\beta)$, and hence releases a charge $-(\beta I_A)T/(1+\beta)$, which is equal to the charge of the longest phase but with opposite sign, and releases an energy equal to

$$(\beta I_A)^2 RT / (1 + \beta). \tag{4}$$

In this way, the total charge released during the entire single period of the asymmetrical wave equals zero, which is a prerequisite for avoiding unwanted low-frequency effects such as neurostimulation and electrolysis.

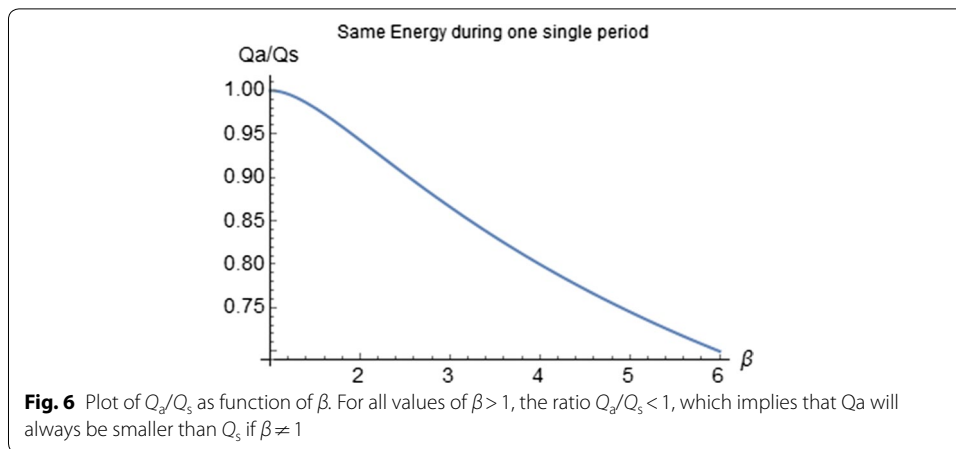
The total energy E_A released during the entire single period of the asymmetrical wave now equals

$$E_A = (I_A)^2 RT \beta, \tag{5}$$

as can be seen by adding the expressions (3) and (4) above.

Gain factor for asymmetrical wave to enforce equal energy for symmetrical and asymmetrical wave

As has been indicated above, a controllable gain factor G for the asymmetrical wave can now be used to ensure that $E_A = E_S$, which corresponds to the *first hypothesis* mentioned in “Background”.



As can be seen from combining Eqs. (2) and (5), the demand $E_A = E_S$ entails that the gain factor G must be tuned to

$$G = 1/\sqrt{\beta}. \tag{6}$$

Now that it is ensured that $E_A = E_S$, we can now evaluate the charge Q_A that is released during a *single phase* out of a single period of the *asymmetrical* wave and compare this charge Q_A to the charge Q_S released during a *single phase* out of a single period of the *symmetrical* wave.

Substituting (6) into (2) yields $I_A = I_S/\sqrt{\beta}$, and hence

$$Q_A = I_A(T\beta)/(1 + \beta) = (I_S/\sqrt{\beta})(T\beta)/(1 + \beta). \tag{7}$$

Since Q_S simply equals $Q_S = I_S T/2$, we now have our main result:

$$Q_A/Q_S = ((I_S/\sqrt{\beta})(T\beta)/(1 + \beta))/(I_S T/2) = 2\sqrt{\beta}/(1 + \beta). \tag{8}$$

As can be seen from the plot of $2\sqrt{\beta}/(1 + \beta)$ as a function of $\beta > 1$ (see Fig. 6), we have that

$$Q_A/Q_S = 2\sqrt{\beta}/(1 + \beta) < 1 \quad \text{for all values of } \beta > 1. \tag{9}$$

Therefore, we now reach our main conclusion that:

$$\text{If } E_A = E_S \text{ then } Q_A < Q_S \quad \text{for all } \beta > 1. \tag{10}$$

This conclusion (10) implies that, if the *first hypothesis*, mentioned in “Background”, is fulfilled, i.e., if the lesion using the asymmetrical wave is deeper than the lesion using the symmetrical wave under the condition $E_A = E_S$, then even more energy for the asymmetrical wave, i.e., $E_A > E_S$, would be needed to satisfy the condition $Q_A = Q_S$ for the *second hypothesis*, which makes the lesion from the asymmetrical wave even deeper than the lesion of the first hypothesis.

Therefore we conclude that:

If the *first hypothesis* is fulfilled, then the *second hypothesis* is fulfilled automatically as well.

Received: 20 October 2018 Accepted: 3 June 2019

Published online: 20 June 2019

References

1. Muthalaly RG, John RM, Schaeffer B, Tanigawa S, Nakamura T, Kapur S, Zei PC, Epstein LM, Tedrow UB, Michaud GF, Stevenson WG, Koplan BA. Temporal trends in safety and complication rates of catheter ablation for atrial fibrillation. *J Cardiovasc Electrophysiol*. 2018;29:854–60.
2. Wittkamp FH, van Es R, Neven K. Electroporation and its relevance for cardiac catheter ablation. *JACC Clin Electrophysiol*. 2018;4:977–86.
3. Wittkamp FH, Van Driel VJ, Van Wessel H, et al. Feasibility of electroporation for the creation of pulmonary vein ostial lesions. *J Cardiovasc Electrophysiol*. 2011;22(3):302–9.
4. Wittkamp FH, Van Driel VJ, Van Wessel H, et al. Myocardial lesion depth with circular electroporation ablation. *Circ Arrhythmia Electrophysiol*. 2012;5(3):581–6.
5. van Driel VJ, Neven K, van Wessel H, Vink A, Doevendans PAFM, Wittkamp FHM. Low vulnerability of the right phrenic nerve to electroporation ablation. *Heart Rhythm*. 2015;12(8):1838–44.
6. Van Driel VJ, Neven KGEJ, Van Wessel H, et al. Pulmonary vein stenosis after catheter ablation electroporation versus radiofrequency. *Circ Arrhythmia Electrophysiol*. 2014;7(4):734–8.
7. Neven K, van Driel V, van Wessel H, van Es R, Doevendans PA, Wittkamp F. Myocardial lesion size after epicardial electroporation catheter ablation after subxiphoid puncture. *Circ Arrhythmia Electrophysiol*. 2014;7(4):728–33.
8. Du Pré BC, Van Driel VJ, Van Wessel H, et al. Minimal coronary artery damage by myocardial electroporation ablation. *Europace*. 2013;15(1):144–9.
9. Chang DC, Reese TS. Changes in membrane structure induced by electroporation as revealed by rapid-freezing electron microscopy. *Biophys J*. 1990;58(1):1–12.
10. Neven K, Van Driel V, Van Wessel H, Van Es R, Doevendans PA, Wittkamp F. Epicardial linear electroporation ablation and lesion size. *Heart Rhythm*. 2014;11(8):1465–70.
11. Neven K, Van Es R, Van Driel V, Van Wessel H, Fidder H, Vink A, Doevendans P, Wittkamp F. Acute and long-term effects of full-power electroporation ablation directly on the porcine esophagus. *Circ Arrhythmia Electrophysiol*. 2017;10:1–8.
12. Krassowska W, Filev PD. Modeling electroporation in a single cell. *Biophys J*. 2007;92:404–17.
13. Arena CB, Sano MB, Rossmeisl JH, Caldwell JL, Garcia PA, Rylander MN, Davalos RV. High-frequency irreversible electroporation (H-FIRE) for non-thermal ablation without muscle contraction. *Biomed Eng Online*. 2011;10:102.
14. Konings MK. Asymmetric balanced waveform for AC cardiac irreversible electroporation. US Patent Application WO2016180934.
15. Prado LN, Goulart JT, Zoccoler M, Oliveira PX. Ventricular myocyte injury by high-intensity electric field: effect of pulse duration. *Gen Physiol Biophys*. 2016;35:121–30.
16. Bronzino JD. *The biomedical engineering handbook*. 2nd ed. Boca Raton: CRC Press; 2000.
17. Golberg A, Yarmush ML. Nonthermal irreversible electroporation: fundamentals, applications, and challenges. *IEEE Trans Biomed Eng*. 2013;60(3):707–12.
18. Son RS, Smith KC, Gowrishankar TR, Vernier PT, Weaver JC. Basic features of a cell electroporation model: illustrative behavior for two very different pulses. *J Membr Biol*. 2014;247:1209–28.
19. Loh KP, van Es R, Groen MH, Neven K, van Driel VJ, van Wessel H, Doevendans PA, Wittkamp FH. Pulmonary vein isolation by irreversible electroporation: first-in-human experience (abstr). *Heart Rhythm*; 2019:S-AB26-02.
20. Stewart MT, Haines DE, Verma A, Kirchhof N, Barka N, Grassl E, Howard B. Intracardiac pulsed field ablation: proof of feasibility in a chronic porcine model. *Heart Rhythm*. 2019;16(5):754–64.

Publisher's Note

Springer Nature remains neutral with regard to jurisdictional claims in published maps and institutional affiliations.

Ready to submit your research? Choose BMC and benefit from:

- fast, convenient online submission
- thorough peer review by experienced researchers in your field
- rapid publication on acceptance
- support for research data, including large and complex data types
- gold Open Access which fosters wider collaboration and increased citations
- maximum visibility for your research: over 100M website views per year

At BMC, research is always in progress.

Learn more biomedcentral.com/submissions

